Raman imaging of human macular pigments

Werner Gellermann,* Igor V. Ermakov, and Robert W. McClane

Department of Physics and Dixon Laser Institute, University of Utah, Salt Lake City, Utah 84112

Paul S. Bernstein

Department of Ophthalmology and Visual Sciences, Moran Eye Center, University of Utah School of Medicine, Salt Lake City, Utah 84132

Received December 19, 2001

We have imaged the spatial distribution of macular carotenoid pigments (MPs) in the human retina, employing Raman spectroscopy. Using excised human eyecups as initial test samples and resonant excitation of the pigment molecules with narrow-bandwidth blue light from a mercury arc lamp, we record Raman images originating from the carbon–carbon double-bond stretch vibrations of the molecules. Preliminary Raman images reveal significant differences in the MPs of different samples in regard to absolute levels as well as spatial variation. This technique holds promise as a method of rapid screening of MPs in large populations at risk for vision loss from age-related macular degeneration, a leading cause of blindness. © 2002 Optical Society of America

OCIS codes: 170.3880, 330.4300, 170.5660.

Over the past few years there has been increasing interest in studying the role of macular carotenoid pigments (MPs) in the human retina. Composed of the carotenoid species lutein and zeaxanthin, these pigments are concentrated in the macula lutea, an ~5-mm-diameter region of the retina that is essential for highest visual acuity and color vision. The MPs may be of fundamental importance in the treatment and prevention of age-related macular degeneration,[1,2] a leading cause of blindness. These pigments absorb light in the blue-green spectral range and are thought to act as filters attenuating photochemical damage and (or) image degradation caused by the highly phototoxic effect of blue-green light components reaching the retina. In addition, it is speculated that MPs may play a protective role as free radical scavenging antioxidants.

To facilitate age-related macular degeneration research, a noninvasive, reliable, and objective method for measuring MPs in the living human macula is needed. Currently the most commonly used noninvasive method of measuring MP levels is a psychophysical heterochromatic flicker photometric test involving color-intensity matching of a light beam aimed at the fovea and another aimed at the perifoveal area.[3,4] However, this method is subjective and time intensive, and it requires an alert, cooperative subject with good visual acuity. Its repeatability depends on the understanding by the subject of the task involved. Thus, the usefulness of this method for assessing MP levels in the elderly population most at risk for age-related macular degeneration and in subjects with macular pathologies is severely limited. Nevertheless, researchers have used flicker photometry to investigate important questions such as variations of MP density with age and diet. In a recent flicker photometry study, for example, the MP density was found to increase slightly with age,[5] whereas two other studies found the opposite trend[6,7] and one study found no change.[8]

Several groups have demonstrated objective methods for detection of MPs based on spectral fundus reflectance[9–13] and autofluorescence.[8] In one variation of these methods, the reflectance across the visual spectrum is measured and estimates of MP concentrations are obtained from a fit of the measured spectra with calculated spectra derived from a detailed optical model for foveal reflection and absorption.[10] In imaging variations of this technique, an imaging fundus reflectometer[11] or a modified scanning laser ophthalmoscope is used to generate reflectance maps.[12,13] Scanning laser ophthalmoscope measurements of MP have been shown to provide more-reliable results than spectral fundus reflectance or psychophysical measurements.[10]

Recently we demonstrated a novel optical approach to *in vivo* detection of MP based on resonance Raman scattering.[14,15] The technique is rapid, sensitive, specific, and highly repeatable in subjects with a wide range of ocular pathologies as long as they still have central fixation (20/80 vision or better).[15] In a first clinical trial, involving over 100 volunteer subjects, Raman detection revealed that MP levels are significantly lower in eyes with macular degeneration relative to age-matched normal eyes, indicating that low levels of lutein and zeaxanthin may represent a pathogenic risk factor.[15] In this Letter we present our first results on extending Raman detection to an imaging mode. Potentially, this method could be used in population studies and give insight into individual variations in the spatial profiles of MP distributions as well as the total amount of MP.

Lutein and zeaxanthin carotenoid pigments are polyenelike molecules featuring a Raman-active, π-electron conjugated carbon backbone with alternating carbon–carbon double (C=C) and single (C–C) bonds. The electronic absorptions are strong, occur in a broad band (~100-nm width) centered at ~450 nm, and show a resolved vibronic substructure with a spacing of ~1400 cm^{-1}. Because of the ordering of the higher energy levels in these molecules, a fluorescence transition is parity forbidden. This important feature allows one to perform resonance Raman scattering without potentially interfering fluorescence.[14] The

0146-9592/02/100833-03$15.00/0

Raman response of these molecules is characterized by two prominent Stokes lines at 1159 and 1524 cm^{-1}, originating, respectively, from the C–C single-bond and the C=C double-bond stretch vibrations of the conjugated backbone, and a weaker peak at 1008 cm^{-1} originating from methyl side groups.[16] For the construction of an imaging apparatus we chose to detect the C=C double-bond stretch vibration at 1524 cm^{-1} as a measure of MP concentration. This Raman line is the strongest and also has the largest Stokes shift, thus simplifying requirements for spectral separation between laser excitation and Raman line.

The experimental setup is shown schematically in Fig. 1. Light from a mercury arc lamp is routed via a fiber bundle into a light delivery and collection module. Inside the module, the light is sent through a diffuser (not shown), collimated by a condenser lens, L_1, spectrally filtered at 488 nm with a 1-nm bandpass filter, F_1, further filtered via reflection from a notch-type holographic beam splitter, BS, and imaged by a lens L_2 (30-mm focal length) onto an ~4-mm-diameter spot centered on the fovea of the excised eyecup (EC). The blue-filtered excitation light power at the fovea is 320 μW, corresponding to an excitation light intensity of 2.55 mW/cm^2. The light scattered back from the retina is collected by lens L_2, transmitted through the beam splitter, and filtered at the C=C stretch frequency (527 nm in the case of 488-nm excitation). The filtering is achieved with a combination of narrowband band interference filters (F_2 and F_3 with bandwidths of 1 and 10 nm, respectively). Camera lens L_3 is used to image the Raman-scattered light onto the 375 × 241 pixel array of a CCD camera (Santa Barbara Imaging Group, Model ST-6uv; pixel size, 23 × 27 μm), permitting digital image acquisition with 16 bits of gray scale. Filter F_2 is angle tuned to alternately transmit the Raman-scattered light at 527 nm (on-peak position) or to transmit the background light at a wavelength position of 529 nm, just missing the Raman peak (off-peak position). The bandwidth of filter F_2 is chosen so that it matches the bandwidth of the excitation light for maximum Raman signal throughput. Beam splitter BS and filters F_2 and F_3 combine to provide an extinction of 10^{-6} at the Raman excitation wavelength (488 nm).

To generate a Raman image we used the difference between two image data sets. A first data set was obtained with filter F_2 tuned to the on-peak position and another set with the filter tuned to the off-peak position. For both data sets identical exposure times (typically 50 s) and imaging conditions were used. All data sets were processed with software obtained from the National Institutes of Health (NIH Image 1.62), allowing us to display the Raman signal levels received by the CCD pixel array versus spatial position as *en face* maps and (or) as topographical representations (surface plots) in pseudo (false) colors. The spatial resolution of these Raman maps is 50 μm.

Human eyes from donors aged 7–60 years with no known history of ocular pathology were obtained from the local eye bank within 24 h after death, immediately after the corneas had been harvested for transplantation. The iris and lens were removed and the vitreous was left undisturbed. The eyecup was placed in a hemispherical holder so that its natural shape would be preserved, and eyes with discernable ocular pathology or postmortem artifacts (e.g., hemorrhages, retinal detachment, macular holes) were rejected. We measured a total of 12 excised postmortem eye cups, all of which yielded significantly varying Raman images. One example from a 41-year-old male is shown in Fig. 2(a) as an *en face* map and in Fig. 2(b) as a surface plot to emphasize MP topology. Raman signal strengths are coded according to the color scale shown on the left-hand side of Fig. 2. MP levels vary by at least an order of magnitude when the noise floor and

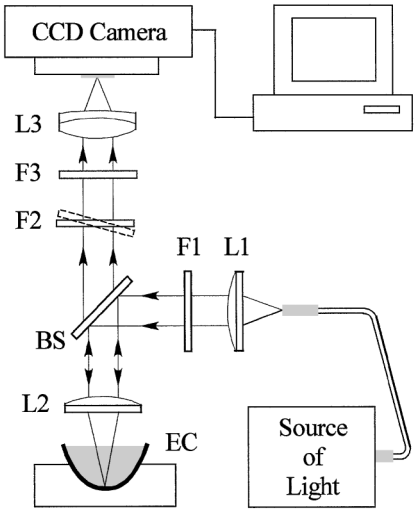

Fig. 1. Experimental setup used for Raman imaging. See text for definitions.

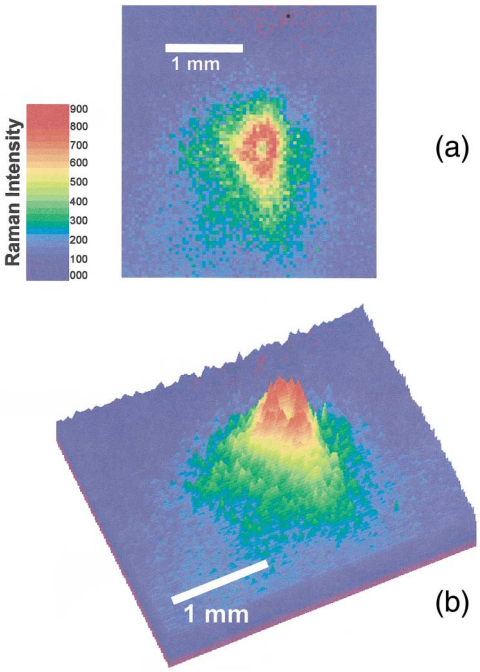

Fig. 2. (a) False-color, *en face* Raman image of MP distribution in the macular region of an excised human eyecup. (b) Corresponding surface plot emphasizing the topology of the MP distribution. Note the central hole in the MP distribution.

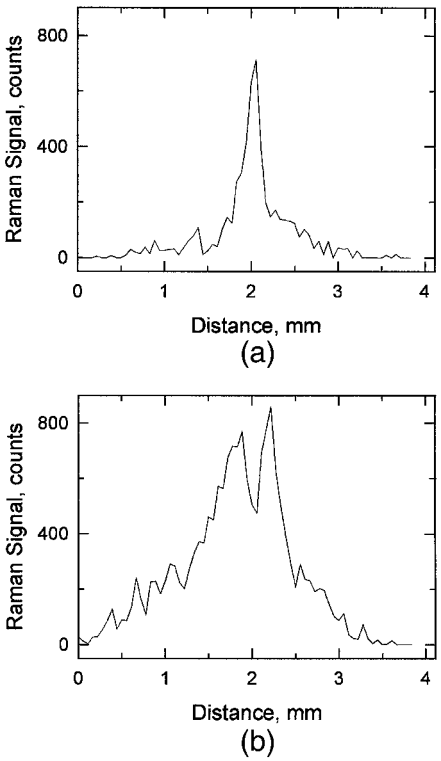

Fig. 3. Line scans of MP distributions obtained by plotting Raman intensities along a line running through the center of the MP distributions and emphasizing differences in the shape and width of individual MP distributions. (a) Line scan corresponding to the MP distribution of the second eyecup. (b) Line scan of the MP distribution of Fig. 2 (first eyecup).

the maxima of the distribution are compared. The Raman images for this eyecup clearly reveal an asymmetric, cone-shaped pigment distribution, with high pigment levels concentrated over a small-diameter central area (FWHM, ~1 mm) and rapidly decreasing levels toward the wings of the cone. The center of the distribution appears to have an ~250-μm-diameter depletion in the pigment density with a hole depth of roughly half the peak pigment concentration. Other eyecups differed in spatial widths of MP, symmetry, and absolute levels. To support this conclusion we compare in Fig. 3 two line plots of MP distributions obtained from the measured *en face* images by plotting the pixel intensities along a line running through the center of the distributions. Figure 3(a) displays the line plot corresponding to the MP distribution of a second eyecup; Fig. 3(b), the line plot of the first eyecup (MP distribution of Fig. 2). Compared with the first eyecup, the second example reveals a much narrower distribution (FWHM, ~250 μm, corresponding to an approximately fourfold reduction in width) and no central hole.

Our Raman image results appear to be in agreement with results published by other groups in relation to MP distributions in healthy living retinas. These include scanning laser opthalmoscope measurements,[13] where drastic individual variations in MP distributions were observed, including the observation of a central hole in pigment levels, and small-stimulus heterochromatic flicker photometry[4] with a reported sevenfold variation of individual MP widths.

In conclusion, we have demonstrated that resonance Raman spectroscopy is capable of imaging physiological MP distributions in human eyecups with a good signal-to-noise ratio by use of Raman excitation with a nonlaser light source. This technique provides detailed information with respect to individual differences in MP absolute levels as well as spatial profiles with micrometer-scale resolution. When this technique is extended to the living human retina, it may permit correlation between MP profiles and macular pathologies.

*Correspondence address, Department of Physics, University of Utah, 115 South 1400 East, Salt Lake City, Utah 84112; e-mail, werner@physics.utah.edu.

References

1. W. Schalch, P. Dayhaw-Barker, and F. M. Barker, in *Nutritional and Environmental Influences on the Eye*, A. Taylor, ed. (CRC, Boca Raton, Fla., 1999).
2. D. M. Snodderly, Am. J. Clin. Nutr. **62,** 1448 S (1995).
3. J. S. Werner, S. K. Donnelly, and R. Kliegl, Vision Res. **27,** 257 (1987).
4. B. R. Hammond, Wooten, and D. M. Snodderly, J. Opt. Soc. Am. A **14,** 1187 (1997).
5. J. S. Werner, M. L. Bieber, and B. E. Schefrin, J. Opt. Soc. Am. A **17,** 1918 (2000).
6. B. R. Hammond and M. Caruso-Avery, Invest. Ophthalmol. Visual Sci. **41,** 1492 (2000).
7. S. Beatty, I. J. Murray, D. B. Henson, D. Carden, H.-H. Koh, and M. E. Boulton, Invest. Ophthalmol. Visual Sci. **42,** 439–446 (2001).
8. F. C. Delori, D. G. Goger, B. R. Hammond, D. M. Snodderly, and S. A. Burns, J. Opt. Soc. Am. A **18,** 1212 (2001).
9. D. van Norren and L. F. Tiemeijer, Vision Res. **26,** 313 (1986).
10. T. T. J. M. Berendshot, R. A. Goldbohm, W. A. A. Kloepping, J. van de Kraats, J. Van Norel, and D. van Norren, Invest. Ophthalmol. Visual Sci. **41,** 3322 (2000).
11. P. E. Kilbride, K. R. Alexander, M. Fishman, and G. A. Fishman, Vision Res. **29,** 663 (1989).
12. D. van Norren and J. van de Kraats, Vision Res. **29,** 1825 (1989).
13. A. A. Elsner, S. A. Burns, E. Beausencourt, and J. J. Weiter, Invest. Ophthalmol. Visual Sci. **39,** 2394 (1998).
14. I. V. Emakov, R. W. McClane, W. Gellermann, and P. S. Bernstein, Opt. Lett. **26,** 202 (2001).
15. W. Gellermann, I. V. Ermakov, M. R. Ermakova, R. W. McClane, D.-Y. Zhao, and P. S. Bernstein, "*In vivo* Raman measurement of macular carotenoid pigments in the young and the aging human retina," J. Opt. Soc. Am. A (to be published).
16. Y. Koyama, I. Takatsuka, M. Nakata, and M. Tasumi, J. Raman Spectrosc. **19,** 37 (1988).